ICAS 2016
30th Congress of the International Council of the Aeronautical Sciences

THE RESEARCH AND VALIDATION OF GLOBAL SKIN FRICTION FIELDMEASUREMENT BASED ON FLUORESCENT OIL FILM

Hong Wei Wang, Beijing; Zhan Huang, Lang Li, Lian feng Wei, Hong Liang Xiong
China Academy of Aerospace Aerodynamics, Beijing, China

Keywords: *skin friction; fluorescent oil film; integral minimization; variation; riblets*

Abstract

Skin friction is one of the most important skin factors in aerodynamics and fluid dynamics along with skin pressure and temperature, though it is very hard to measure exactly. The skin friction measurement based on fluorescent oil film has been developed by its advantage of global and direct measurement compared with traditional ways which were single point or indirect. The governing equation of fluorescent oil film, which express the relationship between the oil film thickness and skin friction, was established. When the oil film thickness is converted to image grayscale, the thin oil film equation can be projected onto the image plane in order to establish the temporal and spatial differential equations of the skin friction. In order to solve the skin friction from the equation, the oil film governing equation is simplified and has the same form with the optical flow constraint equation proposed by Horn and Schunck, and then, it can be solved by introducing additional constraints and using integral minimization approach and variation approach. Then a specific fluorescent indicator excited by ultraviolet light was chosen to develop the fluorescent oil film and a 2K×2K resolution CCD camera was used to record the oil film image. After that a delta wing skin friction measurement experiment was carried out, and high resolution skin friction distribution was acquired and consistent with the theoretical analysis. Here the global skin friction measurement by fluorescent oil film was used by this paper's author to validate the drag reduction effect of the riblet on a laminar flow airfoil in low speed wind tunnel.

1 Introduction

Skin friction, along with skin pressure and temperature, is one of the most important skin factors in aerodynamics and fluid dynamics. For example, skin friction is closely related to the aircraft drag during flying, and the skin friction of large transport aircraft in cruise condition can be up to 50% of total resistance; in the research of turbulent boundary layers, the skin friction could best describe the problem both in assessing the theoretical study or the numerical simulation result; the skin friction field could be used to describe the characteristics and topological structure of the surface flow, and provide a useful approach for understanding the interaction between the flow field and objects. In summary, it has important theoretical and practical significance to research skin friction measurement techniques both in aerodynamic research and engineering application, and lots of techniques have been developed to measure skin friction. For example, wall hot-wire[1], hot-film[2], Preston tube[3], Stanton tube[4], sub-layer fence[5], laser-Doppler[6], shear-stress balance/sensor[7], et al, but most of them are indirect and single point techniques.

Currently, three kinds of techniques can be used to measure skin friction global: Shear Sensitive Liquid Crystal(SSLC)[8][9][10], Surface Stress Sensitive Film(S3F)[11][12] and Oil Film[13]. As directly detecting the response of skin friction, these techniques could be considered as direct or semi-direct methods.

Here, the Oil film skin friction measurement technique, invented by Tanner and Blows, is based on detecting temporal-spatial

evolution of a thin oil film thickness to determine skin friction. They presented a control volume analysis of a layer of thin oil film on a smooth surface subject to the action of shear stress. For a constant local shear stress, they obtained a simple relation between oil film thickness and skin friction:

$$\tau = \frac{\mu x}{ht} \qquad (1)$$

Here μ is the oil viscosity, t is the time from starting the flow, and x is the coordinate from the oil leading edge in the local shear stress direction. The formula (1) is commonly used as a fundamental relation for an oil film skin-friction measurement. In fact, equation(1) describes an intermediate asymptotic state of the evolution of an oil film, where shear stress is so dominant that other forces, such as pressure gradient, surface tension, and gravity, can be neglected.

Generally, the governing equation, which describes the response of a thin oil film on a surface $X_3 = S(X_1, X_2)$ to the externally applied three- dimensional aerodynamic flow, is given in a form of the summation equation:

$$\frac{\partial h}{\partial t} + \frac{\partial}{\partial X_i}\left[\frac{\tau_i h^2}{2\mu} - \left(\frac{\partial p_{gas}}{\partial X_i} - \rho g_i\right)\frac{h^3}{3\mu}\right] = 0 \qquad (2)$$

Where h is the oil film thickness, $(i = 1,2)$, $\boldsymbol{\tau} = (\tau_1, \tau_2)$ is the skin friction vector, p is the pressure gradient, μ is the oil viscosity, ρ is the oil density, and g_i is the gravity vector.

The oil film governing equation, which has established the temporal-spatial evolution of a thin oil film thickness, is the foundation to measure skin friction. So, acquiring oil film thickness spatial and temporal varying information is the key step to solve the governing equation.

The interferometer/laser interferometer (Fig. 1) has been developed by Tanner et al to measure the thickness of a thin oil film at a particular location and been used widely[14]. Among the work of Naughton and Sheplak[15], image-based interferometer oil film measurement was applied in points, lines and regions of surface. Brown and Naughton[16] attempted to recover a global skin friction field as an inverse problem by solving the oil film equation on an oil film domain. But in order to obtain necessary reflection characteristics, the interferometer techniques requires the experiment models having smooth reflective surfaces with special materials while most aerodynamic test models cannot meet this requirement; on the other hand, the interferometer technique also cannot obtain high resolution and complex distribution skin friction.

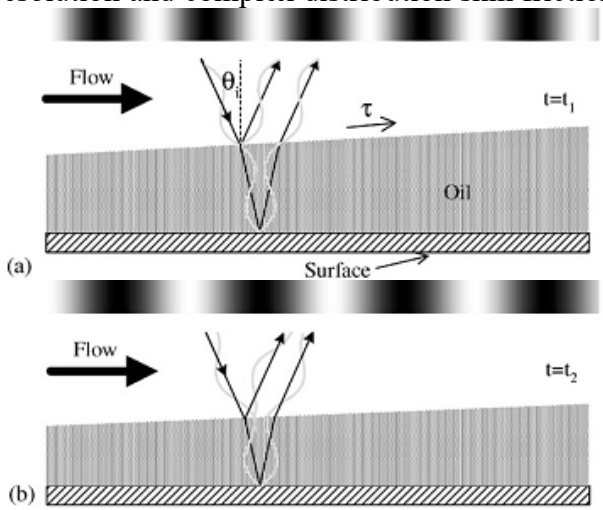

Fig. 1. Measuring the thickness of a thin oil film by interferometer technique

The global extension of a luminescent oil film skin friction measurement was originally proposed by Liu and Sullivan[17]. They used is silicone oil doped with luminescent molecules as luminescent oil. Since the luminescent intensity is proportional to the oil film thickness for a thin oil film, thickness measurement is converted to luminescence measurement which is much easier and more robust against noise.

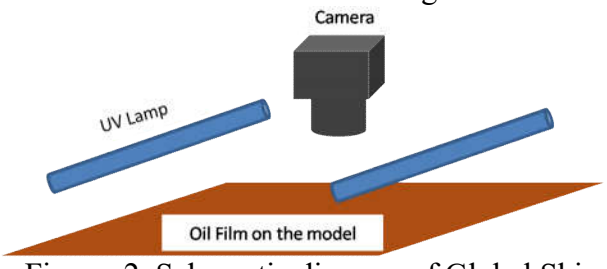

Figure. 2. Schematic diagram of Global Skin Friction Measurement based on Fluorescent Oil Film

When the oil film thickness is converted to image grayscale, the thin oil film equation can be projected onto the image plane to establish the temporal and spatial differential equations of the skin friction. In order to solve the skin

friction from the equation, the oil film governing equation is simplified by Liu et al and then has the same form with the optical flow constraint equation proposed by Horn and Schunck[18] which has been solved by means of integration minimization combined with smoothness constraint condition.

2 Algorithm of Global Skin Friction Measurement based on Fluorescent Oil Film

Based on the governing equation proposed by Tanner and Blows, when a thin luminescent oil film is applied to a surface, the luminescent emission intensity I under excitation is proportional to the oil film thickness and the excitation intensity.

$$I(X_1,X_2)=\alpha I_{excitation}(X_1,X_2)h(X_1,X_2) \tag{3}$$

Where $I_{excitation}(X_1,X_2)$ is the excitation intensity, and Hereinafter referred to as I_{ex}, and α is the coefficient proportional to the quantum efficiency of seeded luminescent molecules. Substitution of equation (3) into equation (2) yields

$$\frac{\partial}{\partial t}\left(\frac{I}{I_{ex}}\right)+\frac{\partial}{\partial X_i}\left[\begin{array}{l}\dfrac{\tau_i}{2\mu}\left(\dfrac{I}{I_{ex}}\right)^2- \\ \dfrac{1}{3\mu\alpha^2}\left(\dfrac{\partial p}{\partial X_i}-\rho g_i\right)\left(\dfrac{I}{I_{ex}}\right)^3\end{array}\right]=0 \tag{4}$$

Because there is one correspondence mapping between the image plan (x_1,x_2) and the oil film surface $X_3=S(X_1,X_2)$, when the image plan is parallel with the oil film surface, the following equation holds projection transformation

$$x_\gamma-x_{\gamma,\nabla}=\lambda X_\gamma \qquad (\gamma=1,2) \tag{5}$$

Where λ can be simplified as constant, and $x_{\gamma,\nabla}$ is considered as origin point of the image plane, i.e.

$$\frac{\partial}{\partial X_i}=\lambda\frac{\partial}{\partial x_i} \tag{6}$$

Introduce the normalized luminescent intensity and equivalent skin friction

$$g=\frac{I}{I_{ex}} \tag{7}$$

$$\bar{\boldsymbol{\tau}}=\tau g\left(\frac{\lambda}{2\mu\alpha}\right) \tag{8}$$

Equation (4) can be written in the image coordinates

$$\frac{\partial g}{\partial t}+\nabla\bullet\left(g\bar{\boldsymbol{\tau}}\right)=f\left(x_1,x_2,g\right) \tag{9}$$

Where $\nabla=\partial/\partial x_i$ is the gradient operator in the image plane, and the effects of the pressure gradient and gravity f are described by

$$f\left(x_1,x_2,g\right)=\lambda\frac{\partial}{\partial x_i}\left[\left(\lambda\frac{\partial p}{\partial x_i}-\rho g_i\right)\frac{g^3}{3\mu a^2}\right] \tag{10}$$

$(i=1,2)$

Here the measured quantity g is mapped onto the image plane. When the radiometric responsive function of a camera is linear, g equals to the normalized gray level in images. Equation (9) is a projected oil film equation for luminescent oil film. Because of introducing the equivalent skin friction $\bar{\boldsymbol{\tau}}$, equation (9) has the same form as the generic projected motion equation for various flow visualizations, and can be solved by optical flow method.

When the spatial variation of skin friction is small ($\partial\bar{\tau}_i/\partial x_i<<1$) and the effects of pressure gradient and gravity can be neglected ($f<<1$), equation (9) can be approximated by a simpler equation which has the same form as the optical flow constraint equation proposed by Horn and Schunck.

$$\frac{\partial g}{\partial t}+\nabla\bullet\left(g\bar{\boldsymbol{\tau}}\right)=0 \tag{11}$$

To determine the equivalent skin friction field $\bar{\boldsymbol{\tau}}=\left(\bar{\tau}_1,\bar{\tau}_2\right)$, equation (11) alone is not sufficient for determining the two unknown skin friction components, and thus additional constraints are required. Here, a variational formulation is introduced to solve this problem. A regularization term based on the square summation of the skin friction gradient that was originally proposed by Horn and Schunck for computing optical flow is used here. This smoothness condition ensures that the equivalent skin friction field is locally continuous in all directions. Given g and f, a function with the Horn-Schunck regularization

term for the skin friction field on an image domain Ω is defined as

$$J(\bar{\tau}) = \int_{\Omega} \left(\frac{\partial g}{\partial t} + \nabla \bullet (g\bar{\boldsymbol{\tau}}) \right)^2 dx_1 x_2 + \alpha \int_{\Omega} \left(|\nabla \bar{\tau}_1|^2 + |\nabla \bar{\tau}_2|^2 \right) dx_1 x_2 \quad (12)$$

The Lagrange multiplier α should be suitably selected. To minimize $J(\bar{\tau})$, the Green's theorem and the Neumann condition $\partial\bar{\boldsymbol{\tau}} / \partial n = 0$ on the domain boundary $\partial\Omega$ are adopted, the Euler-Lagrange equations are given below

$$g \frac{\partial}{\partial x_1} \left[\frac{\partial g}{\partial t} + \nabla \bullet (g\bar{\boldsymbol{\tau}}) \right] + \alpha \nabla^2 \bar{\tau}_1 = 0 \quad (13)$$

$$g \frac{\partial}{\partial x_2} \left[\frac{\partial g}{\partial t} + \nabla \bullet (g\bar{\boldsymbol{\tau}}) \right] + \alpha \nabla^2 \bar{\tau}_2 = 0 \quad (14)$$

Then the iterative method can be used to solve the $\bar{\boldsymbol{\tau}} = (\bar{\tau}_1, \bar{\tau}_2)$ of each point on the image plane.

3 System setting of Global Skin Friction Measurement based on Fluorescent Oil Film

The luminescent oil film is fundamental in the measurement of skin friction, because the oil film thickness and its evolution contain the local information of skin friction. While the fluorescent molecule is an indicator of oil film thickness, its characteristic of excitation light and emission light determine its value in oil film skin friction measurement. Since the fluorescent indicator with significant wavelength difference between excitation light and emission light is mixed in the oil film, and high-pass filter or narrow-band filter is used here to observe emission light to improve the signal to noise ratio.

As a fluorescent indicator, a class of Eu3+ organic complexes' characteristic has been obtained by research. This indicator can absorb the long-wave ultraviolet light nearby 365nm wavelength, and emit red light nearby 612nm wavelength with a high efficiency. When being used to measure the skin friction, the indicator would be blended in specific viscosity silicone oil and fully dispersed.

Tow long-wave UV lamps (600mm, 20W) were used as excitation light source to uniformly illuminate the fluorescent film on the surface of model. An USA Princeton Instrument (PI) ES4020 CCD camera was used as imaging device to achieve the conversion of intensity information of fluorescence oil film to electrical signal. PI ES4020 has a high pixel resolution (2048 pixels × 2048 pixels) and 12 bit quantization precision (i.e. 4096 gray levels) which enable fine spatial measurement and distinguish slight differences in brightness. The camera controller was connected with PC and PI ES4020 by communication cables and in charge of uploading the image information to the PC and accepting the camera control commands from the PC. In order to distinguish the receiving light wavelength (i.e. the emission light wavelength) from excitation light wavelength and improve the signal to noise ratio, a narrow-band filter was required being installed in front of the camera lens. Auxiliary light source and camera fixed and regulation, a number of high-precision linear and angular displacements platform can provide a basis for specific designed experiment light path.

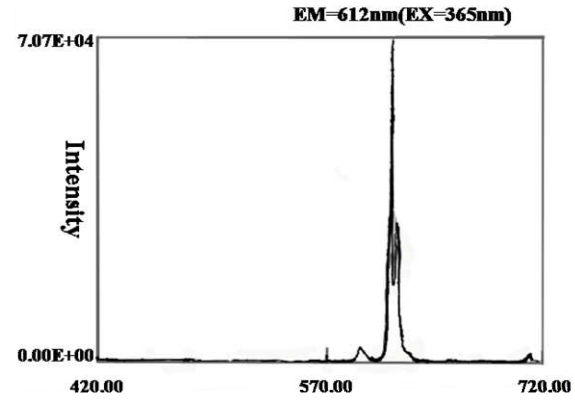

Figure. 3. The fluorescent indicator characteristic of excitation light and emission light

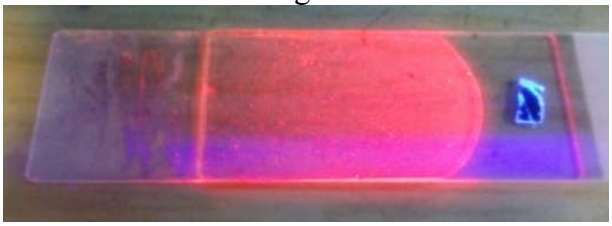

Figure. 4. emission light effect of the fluorescent oil film

4 Global Skin Friction Measurement Validation Test on a Delta Wing

The prototype model is a 65°sweep angle and sharp leading edge delta wing adopted in VFE-2 conference which has 120mm high-line and 112mm bottom length. The experiment was conducted in a small low-speed wind tunnel system which was set up temporarily in the laboratory. The flow speed of wind tunnel test section is controlled by a controllable turbo fan motor and within the range of 1m/s to 20 m/s by regulating the frequency converter.

Figure. 5. The delta model

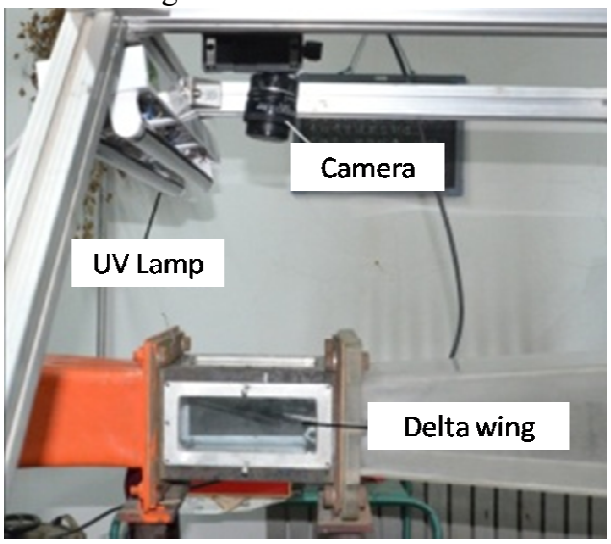

Figure. 6. Test arrangement

The oil film thickness was controlled about 50-80μm; The model attack angle was 10° and the flow velocity was 10m/s; Images of the oil film evolution was captured by the CCD camera which was parallel with the model surface at a frequency of 10Hz; As the fluorescent indicator emit red light near 612nm wavelength, the visible light should be weakened scarcely and a 600nm high-pass filters was added in front of the camera lens. The image data would be transferred to the PC for storage and processing after collected.

Figure. 7. The delta wing in the test section

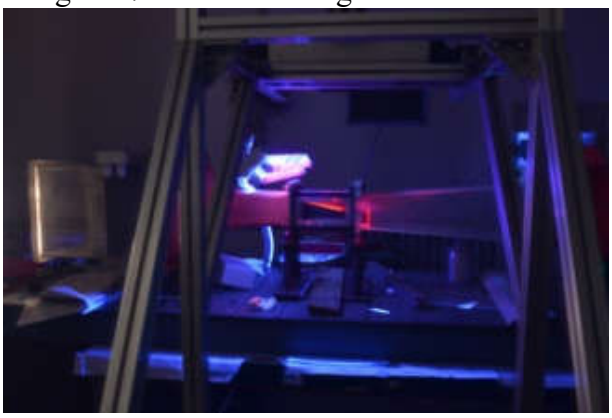

Figure. 8. Performing of the test

Figure. 9. Part of Experimental equipment

5 Validation Test Result and Analysis

The oil film image captured in the experiment is shown in Fig. 10 and the calculated skin friction line is shown in Fig. 11. By comparison the A, B region of Fig. 10 and Fig. 11, it can be indicated that oil film converge too much in the

A, B region so that the oil film thickness increases and impact the local surface flow.

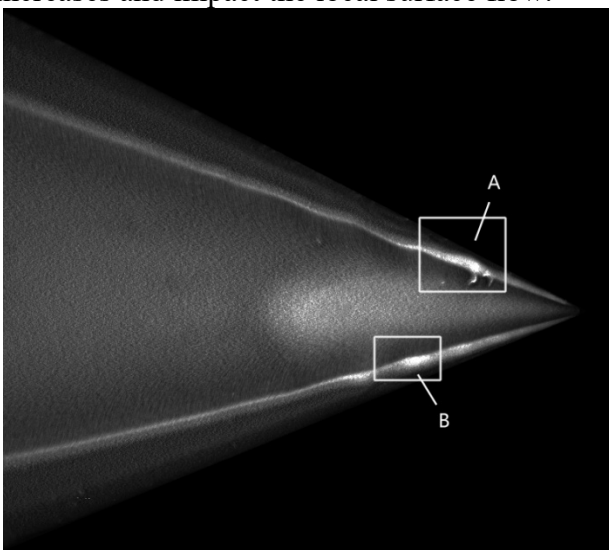

Figure. 10. Image of fluorescent oil film

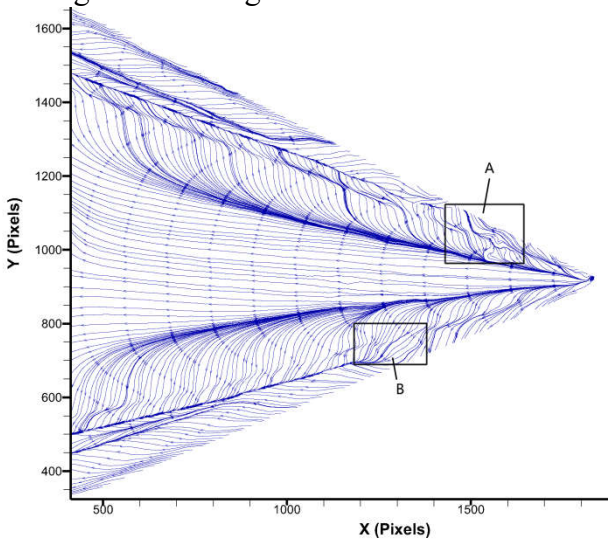

Figure. 11. Skin friction stress line

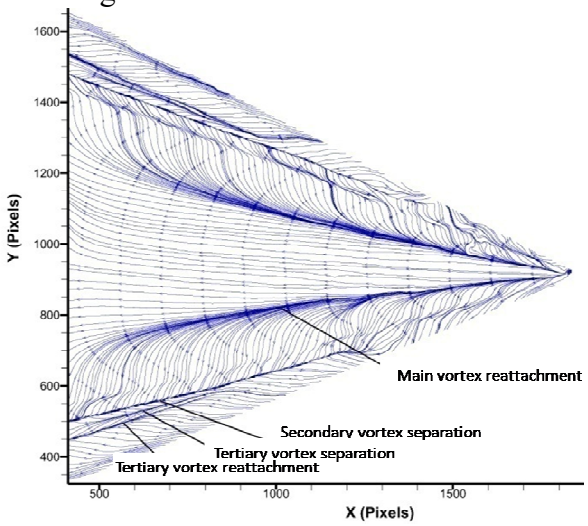

Figure. 12. Detail flags of skin friction stress line

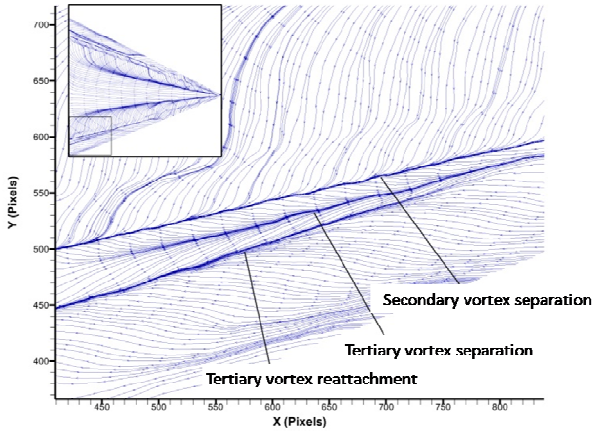

Figure. 13. Local amplification of skin friction stress line

On the other hand, due to the increase of fluorescent indicator, the image overexposes, the results of skin friction is affected and the secondary vortex separation line breaks off here. The most probable cause of this phenomenon is the non-uniform model surface, either machining or bottom paint spraying.

As shown in Fig. 12 and Fig. 13, the calculated skin friction line can reflect the location of main vortex reattachment, secondary vortex separation, and tertiary vortex reattachment.

J.L. Thomas, S.L. Taylor and W.K. Anderson[19] calculated a low speed thin delta wing model upper flow (vortex) field using upwind scheme and finite volume N-S equation. The computation result show the location and skin characteristic of main vortex, secondary vortex and tertiary vortex. As shown in Fig. 14, the separation line Sp of main vortex Cp is beginning at the leading edge of the delta wing, and reattaches at Ap. Because of adverse pressure gradient at Ss, secondary vortex Cs and separation are induced. Similarly, tertiary vortex Ct and separation are induced at St, and the tertiary reattachment line is located at At. The experiment result also was compared with the computation one to approve the location of secondary vortex and tertiary vortex as shown in Fig. 15. Then it could be indicated that the skin friction stress line result in Fig. 12 and Fig. 13 meet the computation result of J.L. Thomas' which is reasonable by the theoretical analysis.

By the solution of fluorescent oil film skin friction above, the oil film thickness can be represented by the image grayscale(i.e.

quantization characterization of g on the image), and then the normalized amplitude of skin friction vector quantitatively mapped to image plane as shown in Fig. 16.

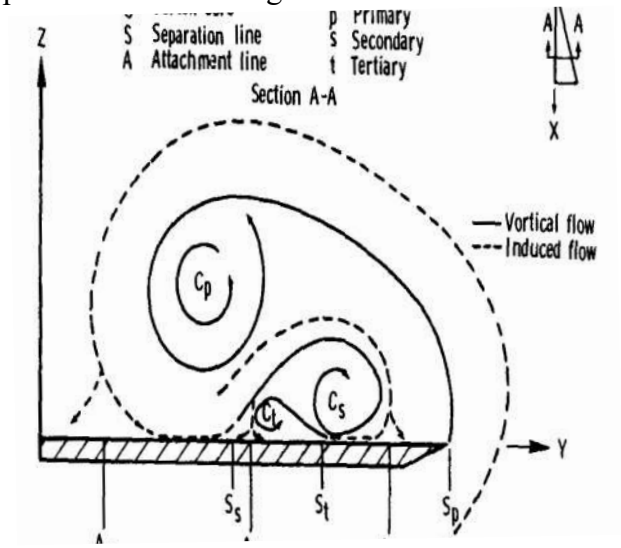

Figure. 14. The location and skin characteristic of main vortex, secondary vortex, and tertiary vortex

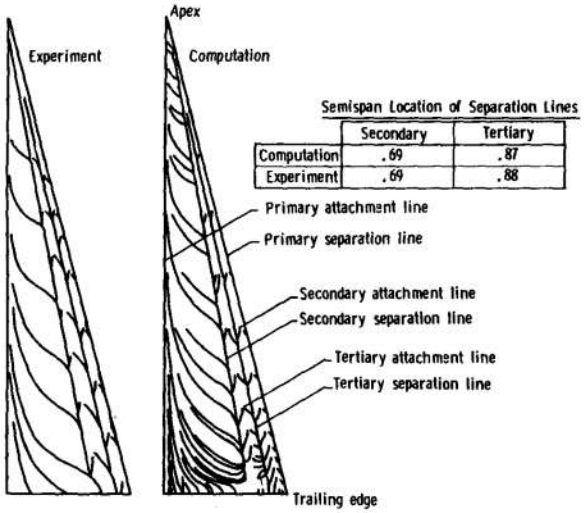

Figure. 15. Comparison of the computation result and experiment result

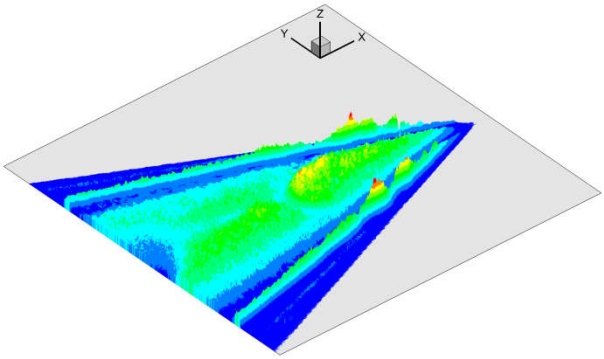

Figure. 16. The normalized amplitude of skin friction

Although this amplitude distribution result is relative, it is very intuitive and effective for analysing global skin friction distribution. As previously described A, B region of the oil film image, the film converge produced thickness abnormal which apparently caused a sharp increase in the amplitude of the skin friction here.

6 Riblets skin friction reduction experiment

For general civil aviation aircraft, the skin friction accounts for about 50% of the total drag, the drag reduction is not only directly related to the performance of civil aviation aircraft, but also indirectly affect the flight cost and environment. Most surface regions of the civil aviation aircraft are in a turbulent flow, so the turbulent boundary layer drag reduction is significant, which has been listed as one of the key technologies of the 21st century aviation by NASA. Study on drag reduction can be traced back to the 1930s, but until the mid-1960s, research work focused on the reduction of the surface roughness, which implicit assumption is that the smooth surface has least resistance. After that, scientists through different flow experiments showed that: the smooth surface is not the best way is to drag reduction as classical Darcy experiment described. After the 1970s NASA Langley Research Center found the riblet grooves along the flow direction can effectively reduce skin friction, which broke the way of thinking that smoother surface had less drag, the drag reduction by riblet grooves became popular subject in turbulent drag reduction.

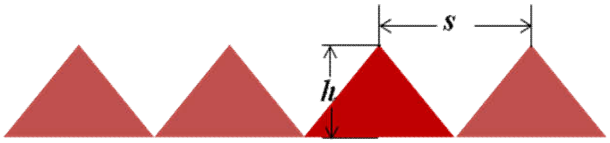

Figure. 17 Typical cross section of riblets film

Many experts and scholars' research agree that the riblet grooves along the flow direction with $h+\leq 25$ and $s+\leq 30$ have drag reduction effect. Here the global skin friction measurement by fluorescent oil film was used by this paper's author to validate the drag reduction effect of the riblet on a laminar flow airfoil in

low speed wind tunnel, where the fluorescent oil film was attached to the smooth film or small rib film downstream of the airfoil model surface as shown in Fig. 18, while the PIV and force balance were also used.

The parameters of the riblets film in this experiment was shown below: Chord=400mm, U∞=20m/s, Re_C~=0.5×10^6, h=0.100mm, s=0.125mm, h+~=7.6, s+~=8.3, which was similar as S. Sundaram's[21] .

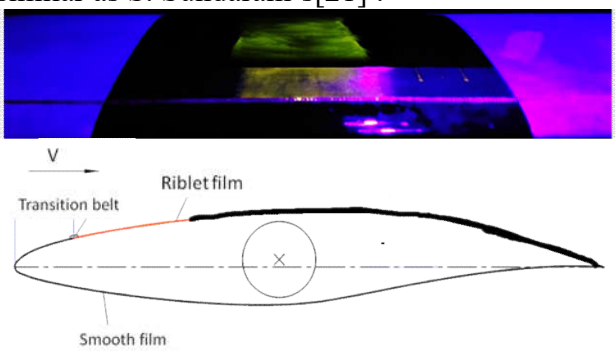

Figure. 18 Schematic diagram of riblets skin friction reduction experiment based on Fluorescent Oil Film

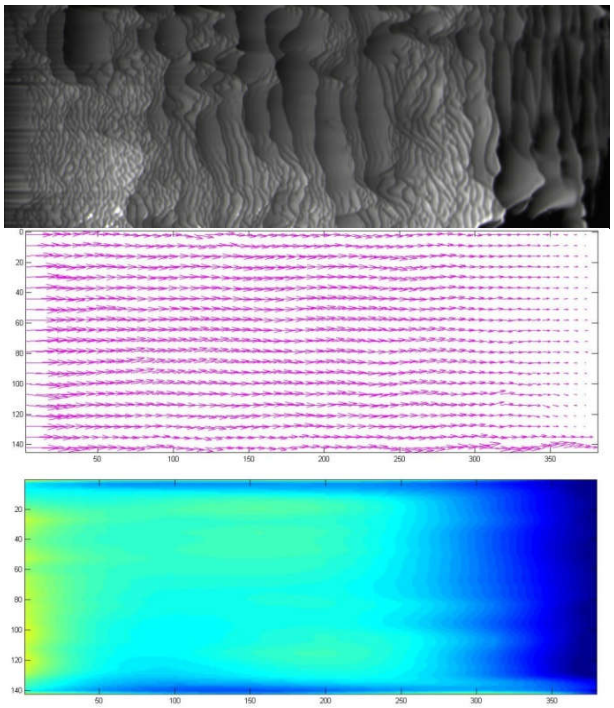

Figure. 19 20m/s oil film image, skin friction vector and magnitude with smooth film(1°)

The 20m/s oil film image, skin friction vector and magnitude with smooth film and riblets film are shown in Fig. 19 and Fig. 20, and the relative magnitude of riblets film and smooth film is shown in Fig. 21. It can be indicated that the relative friction force amplitude of riblets film is reduced obviously compared with the smooth film's. This result and the state of force test results and PIV measurement results are consistent.

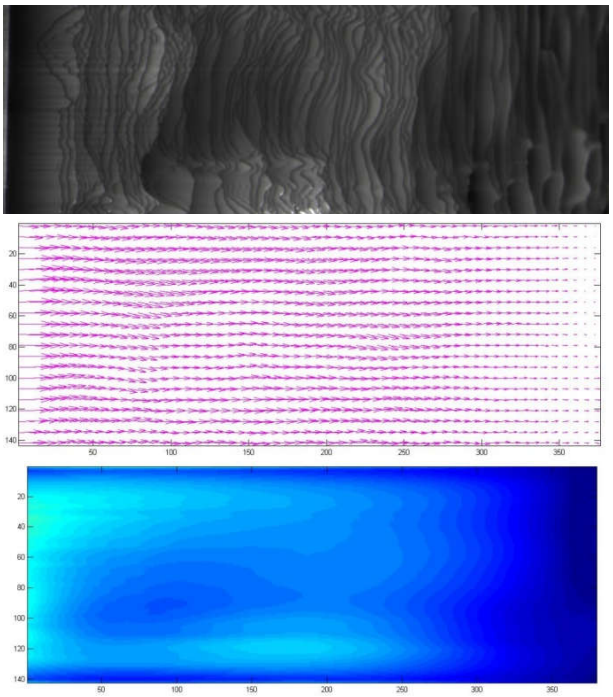

Figure. 20 20m/s oil film image, skin friction vector and magnitude with riblet film(1°)

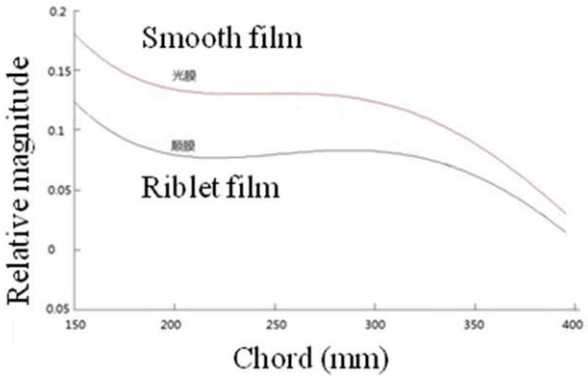

Figure. 21 The Relative magnitude of riblets film and smooth film

7 Conclusion

Global skin friction measurement by fluorescent oil film combines oil-film method and optical flow solution, so it has advantages of global measurement and pixel scale resolution. The model skin friction measurement capacity has been possessed by researched and developed. However, complex models skin friction measurement, efficient fluorescent oil film compound and attached, combined with the

traditional high-precision single point measurement methods could be improved and will be further studied in the future work.

8 Contact Author Email Address

www_whw_cn@163.com

Acknowledgement

This work was supported by National Key Basic Research Program of China (2014CB744801)

References

[1] H H Fernholz, G Janke, et al. “New developments and applications of skin-friction measuring techniques.” [J]. Meas. Sci. Technol, 1996, 7: 1396-1409

[2] Jonathan W. Naughton, Mark Sheplak. “Modern developments in shear-stress measurement.” [J]. Aerospace Sciences, 2002, 38: 515–570

[3] Patel V C. “Calibration of the Preston Tube and Limitation on Its Use in Pressure Gradients.” JFM 1965, 23(1):185-288.

[4] L. A. Wyatt, L.E East. “Low Speed Measure Means of Skin Friction on a Slender Wing.” A. R. C. R&M 3499 Febr, 1966.

[5] Vagt J D, Fernholz H H. “Use of Surface Fences to Measure Wall Shear Stress in Three-Dimensional Boundary Layers.” Aeronautical Quarterly XXIV, 1973:87-91.

[6] Naqwi AA, Reynolds WC. “Dual cylindrical wave laser-Doppler method for measurement of skin-friction in fluid flow.” Tech. Rep. Report No. TF-28, Stanford University,1987.

[7] Schmidt MA, Howe RT, Senturia SD, Haritonidis JH. “Design and calibration of a micro fabricated floating-element shear-stress sensor.” Trans Electron Dev 1988;ED-35:750–7.

[8] Gaudet L, Gell TG. “Use of liquid crystals for qualitative and quantitative 2-D studies of transition and skin-friction.” ICIASF ’89, 13th International Congress on Instrumentation in Aerospace Simulation Facilities, Gottingen, Germany, Institute of Electrical and Electronics Engineers, 1989.

[9] Bonnet P, Jones TV, McDonnell DG. “Shear-stress measurement in aerodynamic testing using cholesteric liquid crystals.” Liq Cryst 1989;6(3):271–80.

[10] Reda, D. C., Wilder, M. C., Mehta, R. D., and Zilliac, G., “Measurement of Continuous Pressure and Shear Distributions Using Coating and Imaging Techniques,” AIAA Journal, Vol. 36, No. 6, 1998, pp. 895–899.

[11] Fonov, S. D., Jones, G., Crafton, J., Fonov, V., and Goss, L., “The Development of Optical Technique for the Measurement of Pressure and Skin Friction,” Measurement Science and Technology, Vol. 17, No. 6, 2006, pp. 1261–1268.

[12] Crafton, J. W., Fonov, S. D., Jones, G., and Fonov, V. S., “Optical Measurements of Pressure and Shear in a Plasma,” AIAA Paper 2005-5006, June 2005.

[13] Tanner LH, Blows LG. “A study of the motion of oil films on surfaces in air flow, with application to the measurement of skin-friction.” J Phys E 1976;9(3):194–202.

[14] Monson DJ, Driver DM, Szodruch J. “Application of a laser interferometer skin-friction meter in complex flows. ” Proceedings of the ICIASF, IEEE Publication 81CH1712-9. New York: IEEE, 1981. p. 232–43.

[15] Naughton, J. W., and Sheplak, M., “Modern Developments in Shear-Stress Measurement,” Progress in Aerospace Sciences, Vol. 38, Nos. 6–7, 2002, pp. 515–570.

[16] Brown, J. L., and Naughton, J. W., “The Thin Oil Film Equation,” NASA TM 1999-208767, March 1999.

[17] Liu, T., and Sullivan, J. P., “Luminescent Oil-Film Skin Friction Meter,” AIAA Journal, Vol. 36, No. 8, 1998, pp. 1460–1465.

[18] Horn B K P. Schunck B G. “Determining optical flow, ” [J]. Artificial Intelligence 1981. 17 :185~203

[19] J .L.Thomas , S.L.Taylor and W.K. Anderson, “Na vier-Stokes Computations of Vortical Flows Over Low Aspect RatioWings, ” AIAA-87-0207

[20] Walsh M J. Riblets: viscous drag reduction in boundary layers [R]. NASA Technical Report, Virginia, 1990.

[21] Sundaram, S and Vishwanath, PR and Subhaschandar, N (1999) Viscous drag reduction using riblets on a swept wing. AIAA Journal, 37 (7). pp. 851-856.

Copyright Statement